

The use of circular birefringent material as an interstage element of a linear birefringent network

Biswajit Chakraborty

Citation: [Journal of Applied Physics](#) **64**, 2847 (1988); doi: 10.1063/1.341595

View online: <http://dx.doi.org/10.1063/1.341595>

View Table of Contents: <http://scitation.aip.org/content/aip/journal/jap/64/6?ver=pdfcov>

Published by the [AIP Publishing](#)

Articles you may be interested in

[Virtual circular array using material-embedded linear source distributions](#)

Appl. Phys. Lett. **95**, 173503 (2009); 10.1063/1.3257374

[MFL SIGNAL INVERSION USING THE FINITE ELEMENT NETWORK](#)

AIP Conf. Proc. **975**, 633 (2008); 10.1063/1.2902722

[Linear Magnetoacoustic Birefringence in Dysprosium](#)

AIP Conf. Proc. **10**, 764 (1973); 10.1063/1.2947012

[APPARATUS FOR TEACHING PHYSICS: Interference of Birefringent Materials Using Polarized Light](#)

Phys. Teach. **8**, 398 (1970); 10.1119/1.2352660

[Linear and Circular Acoustical Birefringence in Ferroacoustic Resonance](#)

J. Appl. Phys. **37**, 990 (1966); 10.1063/1.1708552

The advertisement features a dark blue background with a film strip graphic on the left. The text is in white and orange. The main headline reads 'Not all AFMs are created equal' in orange, followed by 'Asylum Research Cypher™ AFMs' in white, and 'There's no other AFM like Cypher' in orange. Below this is the website 'www.AsylumResearch.com/NoOtherAFMLikeIt' in white. In the bottom right corner is the Oxford Instruments logo, which consists of the word 'OXFORD' in a large font above 'INSTRUMENTS' in a smaller font, all within a white rectangular border. Below the logo is the tagline 'The Business of Science®' in a small white font.

The use of circular birefringent material as an interstage element of a linear birefringent network

Biswajit Chakraborty

Optics and Optoelectronics Section, Department of Applied Physics, University of Calcutta, 92 Acharya Prafulla Chandra Road, Calcutta 700 009, India

(Received 14 September 1987; accepted for publication 20 May 1988)

In a previous communication the transmission characteristics of both narrow bandpass filters and birefringent band suppression filters (BBSF) have been investigated where a retarder-rotator combination is used at each stage. The tuning procedures of these fixed-type filters have also been studied where the thickness of each retarder plate was the same and the thickness of each rotator plate was the same. In the present paper we first study the variation of intensity transmittance with the variation of number of stages of the previously proposed filter. A simple way of synthesizing a BBSF system by using a number of equal thickness linear retarder plates is also indicated. Lastly we study the transmission characteristics and the tuning procedures of both narrow bandpass filters and birefringent band suppression filters where the retarder and the rotator plates of unequal thicknesses are used for their construction.

I. INTRODUCTION

A stepwise development in the field of birefringent spectral filters has been indicated in a previous communication.¹ The present paper highlights the further studies in the field of birefringent spectral filters by utilizing the ideas of Ref. 1. For the sake of systematic studies we divide the entire paper into three different parts. In Sec. II we study the change in the transmission characteristics due to the change in the number of stages of same systems shown in Ref. 1. Here the filter core is made of a particular combination of retarder plates of equal thickness and rotator plates of equal thickness. A cascaded linear birefringent network having an approximated periodic rectangular amplitude transmittance is also shown as a band-suppression filter system in Sec. II. Section III includes the studies on the transmission characteristics of the birefringent filter systems where the elements of the successive stages get double in thickness like in a Lyot filter. Lastly Sec. IV deals with the birefringent filter systems where the thickness of the elements of the successive stages are different. Here we study the effect of substituting the mechanical rotations of the retarder plates of a linear birefringent network by the frequency-dependent rotations introduced by the interstage rotators. It is instructive to point out at this stage that this paper adheres to the notations and conventions of Ref. 1 unless otherwise stated.

II. BIREFRINGENT FILTER SYSTEM WHERE THE THICKNESS OF EACH RETARDER PLATE IS THE SAME AND THE THICKNESS OF EACH ROTATOR PLATE IS THE SAME

The variation of intensity transmittance T with the variation of wavelength λ of a 14-stage ($n = 14$) narrow bandpass filter is shown in Fig. 1. The plot is obtained with the help of the expressions (11) and (12) of Ref. 1. The filter is tuned at $\lambda_{op} = 509$ nm and the thickness of each interstage quartz rotator plate is 0.44 mm (for $m = 2$). Comparing the T vs λ plot of Fig. 1 with that of a 10-stage narrow bandpass filter [Fig. 2(a), Ref. 1] we find that as the number of stages increase the width of the central maxima decreases along

with the amplitudes of the secondary maximas on both sides of the principal maxima. This situation is particularly interesting because of the fact that in a well-known linear birefringent narrow bandpass filter such as a solc filter, as the number of stages increase, the amplitudes of the secondary maximas on both sides of the principal maxima increase while the width of the principal maxima decreases.

Figure 2 shows the T vs λ curve of a 14-stage birefringent band suppression filter (BBSF) system tuned at $\lambda_{OR} = 509$ nm. This plot is obtained with the help of the expressions (15) and (16) of Ref. 1 and the thickness of each quartz rotator plate is 0.22 mm (for $m = 1$). Comparing the T vs λ curve of Fig. 2 with that of a 10-stage BBSF system [Fig. 2(e), Ref. 1] we find that as the number of stages increase the amplitudes of fluctuations over the pass band of both sides of $\lambda_{OR} = 509$ nm decrease slightly and the width of the rejection band decreases too.

A birefringent band suppression network can also be synthesized by impulse response technique² which uses equal length linear retarder plates as core elements. A five-stage linear birefringent network having an approximated periodic rectangular amplitude transmittance (obtained by a six-term exponential Fourier series and shown in Fig. 3) has been synthesized by the simple synthesis process described by Harris, Ammann, and Chang.³ The absolute an-

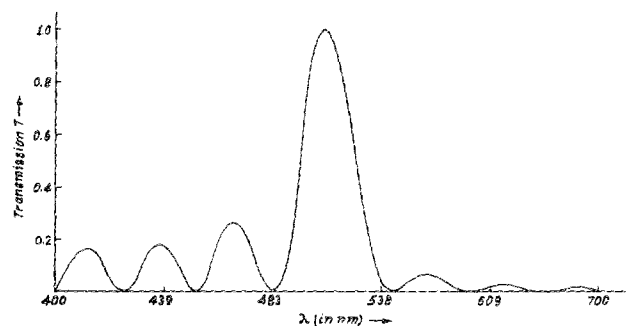


FIG. 1. Transmission curve of a narrow band-pass filter for $n = 14$, $m = 2$, $\lambda_{op} = 509$ nm, and $\theta = 6^\circ 25'$. The thickness of each retarder is the same and the thickness of each rotator is the same.

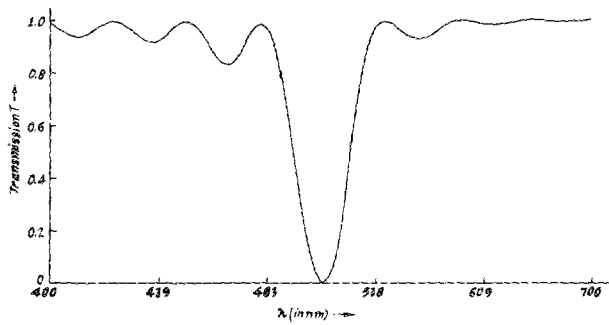


FIG. 2. Transmission curve of a birefringent band suppression filter for $n = 14$, $m = 1$, $\lambda_{0,R} = 509$ nm, and $\theta = 0^\circ$. The thickness of each retarder is the same and the thickness of each rotator is the same.

gles (measured with respect to the x axis) of the first, second, third, fourth, and fifth retarder and the output linear polarizer are $\theta_1 = -21^\circ 36'$, $\theta_2 = -2^\circ 32'$, $\theta_3 = -56^\circ 34'$, $\theta_4 = -110^\circ 37'$, $\theta_5 = -91^\circ 19'$, and $\theta_p = -23^\circ 10'$, respectively. The transmission axis of the input linear polarizer is assumed to be parallel to the x axis (horizontal direction) of a cartesian coordinate system. The normalized intensity transmittance of the five-stage linear birefringent network having an approximated periodic rectangular amplitude transmittance is shown in Fig. 4. The principal rejection wavelength corresponds to $\delta = \pi/2$ or $3\pi/2$ where δ is the frequency-dependent retardance introduced by each linear retarder plate. Although, ideally, full transmission is desirable at each wavelength of the passband, here we note some fluctuations over the passband of the band suppression filter.

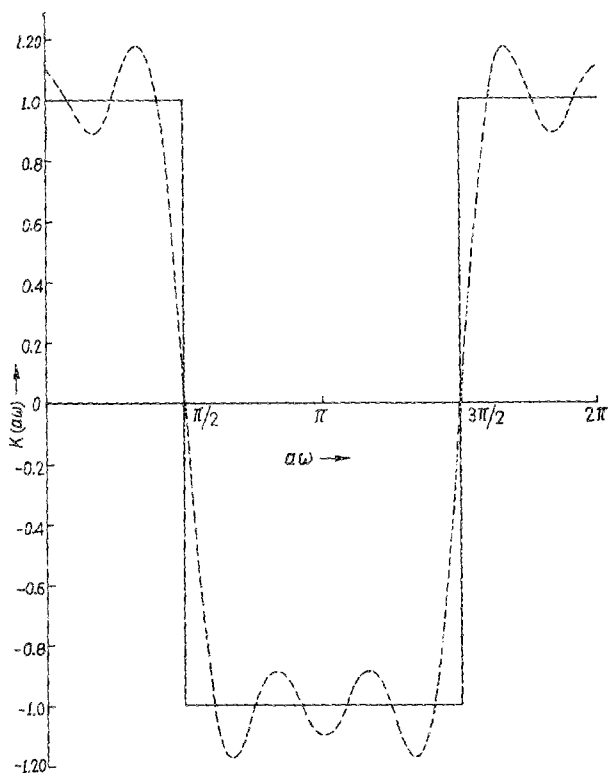


FIG. 3. Plots show the ideal (firm line) and the approximated (dotted line) amplitude transmittance of a five-stage linear birefringent network having a periodic rectangular amplitude transmittance.

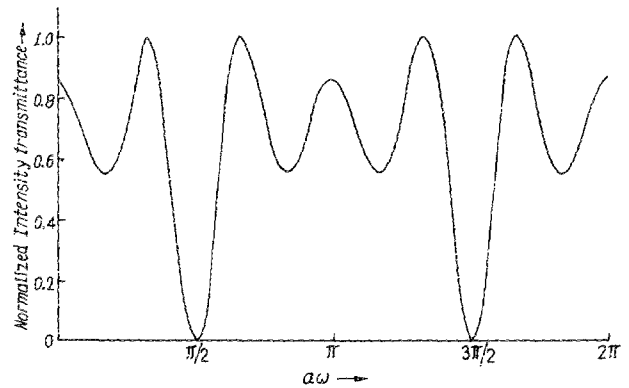


FIG. 4. Normalized intensity transmittance of a five-stage linear birefringent network having an approximated periodic rectangular amplitude transmittance.

By increasing the number of stages the rejection bandwidth can be made narrower and the amplitudes of the ripple over the passband can also be reduced. But as the number of stages increase the number of terms in the approximated amplitude transmittance increases too (the mean square error comes down) while the approximated function shows a large amount of ripple at the point of discontinuity. This causes lowering of the entire pass band in the normalized intensity transmittance curve. Figure 5 shows the normalized intensity transmittance curve of a 13-stage band suppression linear birefringent network, obtained from 14-term exponential Fourier series. The plot shows a lowering of the pass band at the higher wavelength side of the principal rejection wavelength at 448 nm.

III. BIREFRINGENT FILTER SYSTEM WHERE THE ELEMENTS OF THE SUCCESSIVE STAGES DOUBLE IN THICKNESS

We now study the transmission characteristics of both narrow passband filter and birefringent band suppression filter of same arrangements as shown in Fig. 1 of Ref. 1, with the only difference that the elements of the successive stages double in thickness. The generalized expression for the output Jones vector E_o of a n -stage network where the retarder axes are oriented like a n -stage, fan-type solc filter is given by

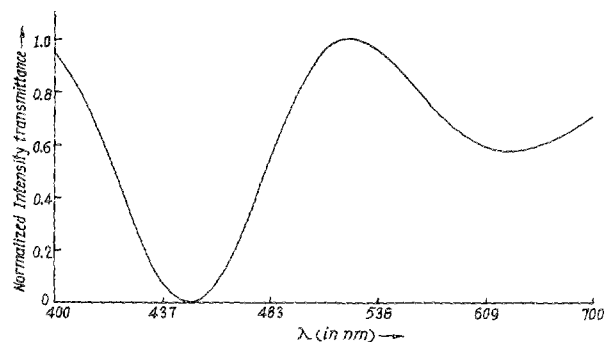


FIG. 5. Normalized intensity transmittance of a 13-stage linear birefringent network having an approximated rectangular amplitude transmittance.

$$E_0 = P_{\text{out}}(0)R(\theta/2)R(n\theta)R(2^{n-1}\alpha - \theta)C(2^{n-1}\delta) \\ \times R(2^{n-2}\alpha - \theta)C(2^{n-2}\delta)\dots R(\alpha - \theta)C(\delta) \\ \times R(-\theta/2)P_{\text{in}}(0)E_i, \quad (1)$$

where

$$E_i = \begin{pmatrix} E_x \\ E_y \end{pmatrix}$$

represents the Jones vector of the input beam and $C(\delta)$, $R(\alpha)$, and $P(0)$ represent the Jones matrices of the retarder, rotator, and linear polarizer, respectively. Here, unlike the cases of Sec. II where the closed-form expressions were used to obtain the intensity transmittance plots, rigorous computer software (multiplication of a series of 2×2 complex matrices) is used to obtain the intensity transmittance values at different wavelengths with the help of expression (1) and with the aid of an IBM 1130 computer. For computational purposes we use Biot's law¹ in order to realize the optical rotation produced by a quartz rotator plate and neglect the dispersion of birefringence of a linear retarder plate due to the reason indicated in Ref. 1.

Plot (a) of Fig. 6 shows the T vs λ curve of a 10-stage network tuned for a narrow bandpass purpose. Here the first rotator (from the left-hand side) rotates the plane of polarization of the principal pass wavelength component through an angle determined by the relation

$$\alpha_{op} = m\pi \left/ \sum_{n=1}^n 2^{n-1} \right., \quad (2)$$

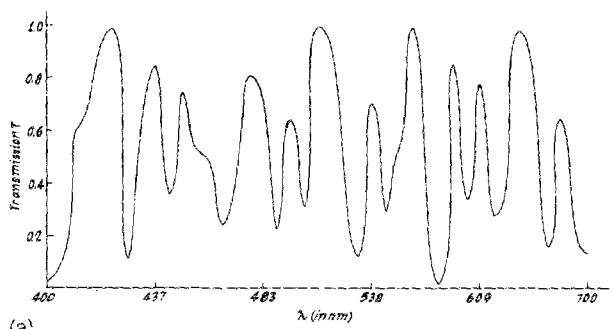
where $m = 1, 2, 3, 4, 5$, etc. For $n = 10$ and $\lambda_{op} = 509$ nm if we choose any value of m between 1 and 19, the thickness of the first few rotators will be impossibly small. So, we prefer to choose $m = 20$ for the computational purpose which determines the thickness of the first rotator as 0.12 mm and the thickness of the last rotator as 6.13 cm. The first retarder [just after $P_{\text{in}}(0)$] introduces a phase difference of 360° at $\lambda_{op} = 509$ nm. Plot (a) of Fig. 6 shows sharp peaks of different amplitudes and shapes where the azimuths of the retarders are arranged like a 10-stage Solc filter (that yields $\theta = 9^\circ$ from $n\theta \approx \pi/2$). At $\lambda_{op} = 509$ nm the intensity transmittance is at its ideal maximum. Plot (b) of Fig. 6 shows the T vs λ curve of the same setup with the only difference that the slow axis of each retarder is parallel to the transmission axes of the polarizers, i.e., $\theta = 0^\circ$. Here obviously the number of retarder is one less than the number of rotator and the first retarder [after the first $R(\alpha)$ from the left-hand side; Fig. 1, Ref. 1] introduces a phase difference of 720° at λ_{op} . Plot (b) of Fig. 6 also shows a number of sharp peaks of different shapes. If now for the 10-stage network the thickness of each retarder is the same and is made to introduce a phase difference of 360° at λ_{op} and the rotators are chosen according to relation (2) (with $m = 20$), then for $\lambda_{op} = 509$ nm we get the T vs λ variation of plots (c) and (d) of Fig. 6 for both $\theta = 9^\circ$ and 0° , respectively. These curves also show an irregular distribution of sharp peaks. A large number of transmission peaks of plot (d) are found to be sharper than those obtained in plots (a), (b), and (c) of Fig. 6.

We now study the T vs λ curves of a fan-type solc filter where the successive retarders double in thickness [substi-

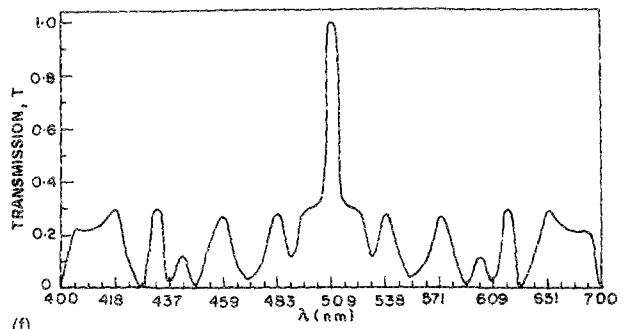
tuting $\alpha = 0$ in expression (1)]. The transmission curves of the six-stage ($n = 6$) and the 10-stage ($n = 10$) filter of this type, tuned at $\lambda_{op} = 509$ nm, are shown in plots (e) and (f) of Fig. 6, respectively. Comparing plot (f) of Fig. 6 with that of a 10-stage fan-type Solc filter [shown in Fig. 2(d) of Ref. 1] we see that the much narrower transmission peak can be obtained at the principal pass wavelength $\lambda_{op} = 509$ nm but the amplitudes of the secondary peaks get higher and the side bands are of irregular shape as the successive stages get doubled in thickness.

With the help of expression (1) we now study the T vs λ curve of a birefringent network where equal thickness rotator plates are used as interstage elements and the retarders of successive stages double in thickness. Here again we retain to original terms and conditions of Ref. 1 in order to find the thickness of each rotator plate. Plots (g), (h), and (i) of Fig. 6 show the T vs λ curves of a 10-stage ($n = 10$) filter of this type tuned at $\lambda_{op} = 509, 453$, and 640 nm, respectively. The curves of plots (g), (h), and (i) are drawn for $m = 2$ and the thickness of the rotators are obtained as 0.60, 0.48, and 1 mm, respectively. The first retarder [just after $P_{\text{in}}(0)$; Fig. 1, Ref. 1] behaves as a full wave plate for the principal pass wavelength and the azimuths of the retarders are arranged like a fan-type Solc filter. Comparing the T vs λ curve of plot (g) with that of plot (f) of Fig. 6 we see that in plot (g) of Fig. 6 the secondary peaks at the higher wavelength side of principal pass are greatly reduced where as the secondary peaks at the lower wavelength side increase. If now the number of stages are decreased to $n = 6$, we get the transmittance curve of plot (j) of Fig. 6 (tuned at $\lambda_{op} = 509$ nm) which, when compared to that of plot (g) of Fig. 6, reveals that the increase in the number of stages decrease the amplitudes of the peaks on the higher wavelength side than on the lower wavelength side of λ_{op} . Again if the thickness of each rotator is changed the T vs λ curve takes the shape (for $n = 10$) shown by plot (k) of Fig. 6. Here we use $m = 4$ and the thickness of each rotator is obtained as 1.22 mm for $\lambda_{op} = 509$ nm. Comparing plot (k) with plot (g) of Fig. 6 we see that the width of primary maxima as well as the number of secondary maxima increase as the thickness of each rotator increases. Plot (l) of Fig. 6 shows the T vs λ curve of a 10-stage (number of the retarder is 9) network where the slow axis of each retarder is parallel to the transmission axes of the polarizers and $m = 2$, $\lambda_{op} = 509$ nm. The first retarder introduces a phase difference of 720° at λ_{op} . Here again we see a number of transmission peaks of different shapes.

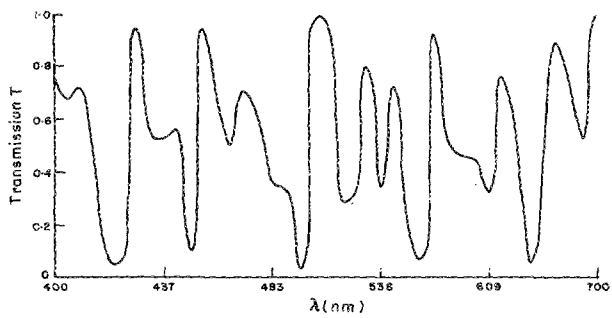
We now present two cases of a 10-stage network tuned at principal rejection wavelength $\lambda_{OR} = 509$ nm at which the value of intensity transmittance is ideally zero. The thickness of each rotator is same and the first retarder introduces a phase difference of 360° at λ_{OR} . Plot (m) of Fig. 6 shows the T vs λ curve of the band suppression network where the axes of the retarders are oriented like a 10-stage Solc filter. Plot (n) of Fig. 6 shows the T vs λ curve of the same network where the slow axis of each retarder is parallel to the transmission axes of the polarizers. In this setup the number of the retarder is one less than the number of rotator, and first retarder introduces a phase difference of 720° at λ_{OR} . In both the cases the thickness of each rotator is obtained as 0.31 mm



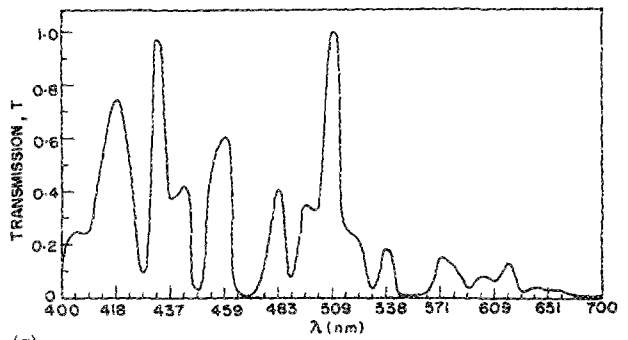
(a)



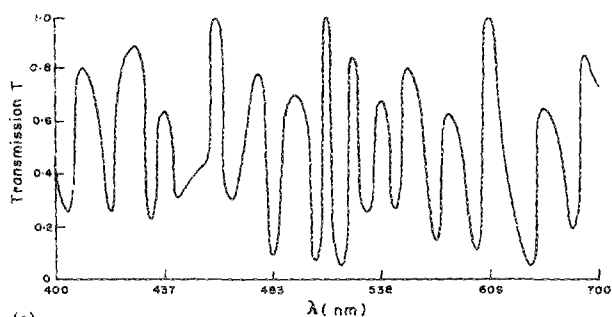
(f)



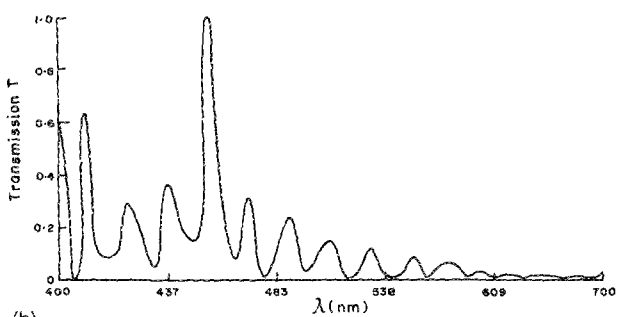
(b)



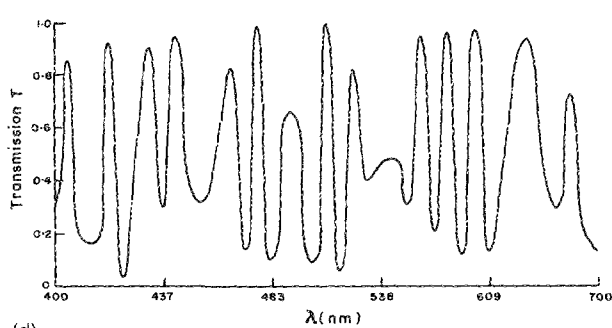
(g)



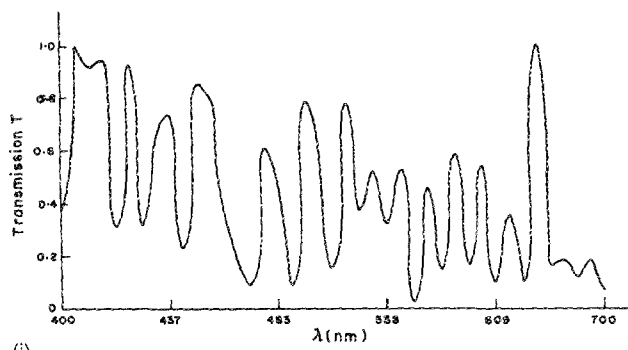
(c)



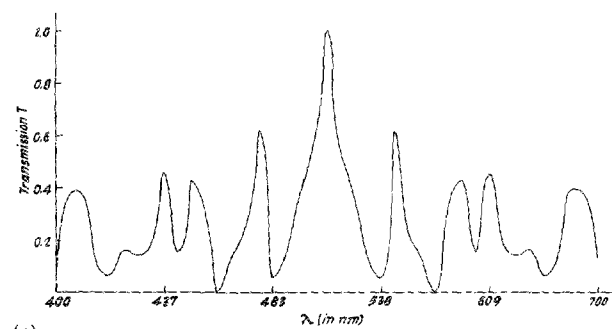
(h)



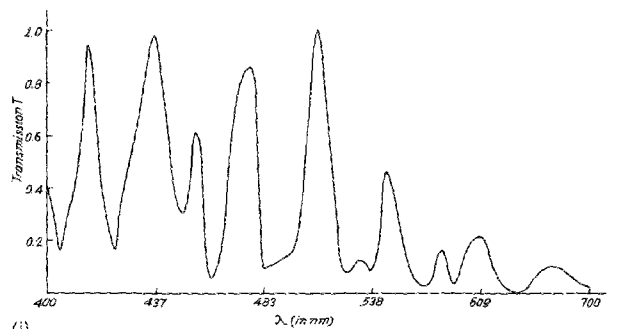
(d)



(i)

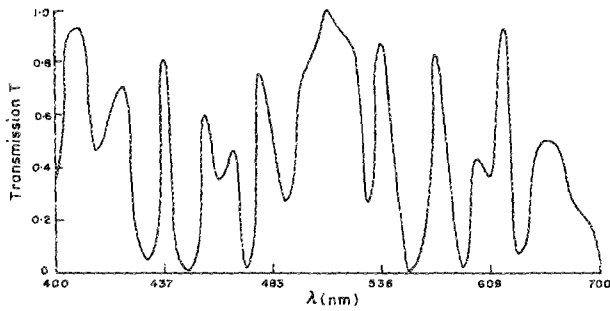


(e)

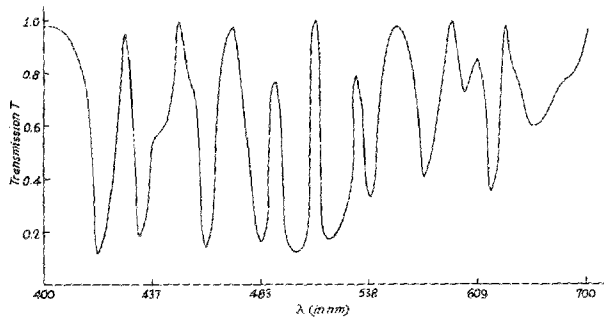


(j)

FIG. 6. Plots (a)–(n) show the transmission curves of the birefringent filter systems where the elements of the successive stages increase in a regular way.



(k)



(l)

FIG. 6. (continued).

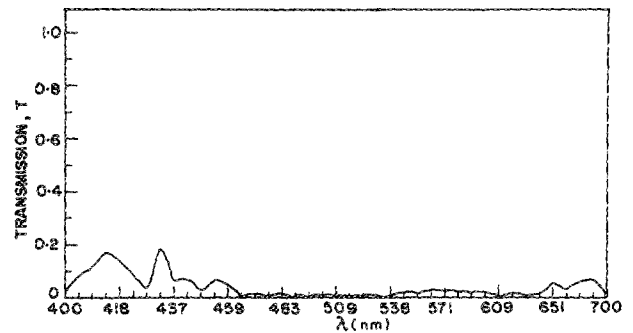
for $m = 1$. It is interesting to note that in plot (m) of Fig. 6 we get a complete suppression over a wide spectral range around λ_{OR} with little transmission at both ends. Plot (n) of Fig. 6 shows large amplitude of fluctuation over the lower wavelength side passband than on the higher wavelength side passband of λ_{OR} . In both the cases discussed above, the fluctuations over the passband of either side of λ_{OR} increase as we take higher value of m or higher number of stages.

IV. BIREFRINGENT FILTER SYSTEM WHERE THE THICKNESS OF EACH RETARDER IS THE SAME AND THE THICKNESSES OF INTERSTAGE ROTATORS ARE DIFFERENT

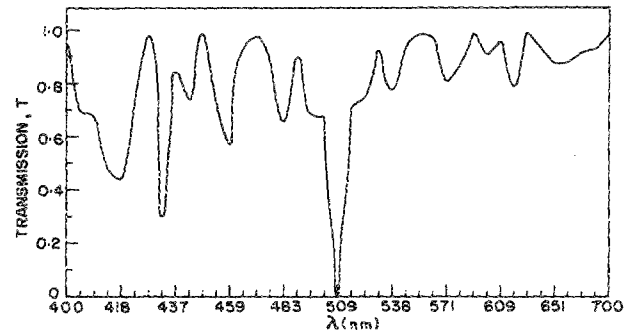
In the preceding sections the spectral intensity transmittance of different types of birefringent filters are studied where the slow axes of different retarders are either arranged by a simple mathematical relation or parallel to the transmission axes of the polarizers. The thickness of different core elements are shown to be the same or increase in a regular way. In the following studies we investigate the effect of substituting the mechanical rotations of the linear retarder plates of a linear birefringent network by the frequency-dependent rotations introduced by the optically active medium.

Figure 7 shows a five-stage linear birefringent network. Following Jones formalism the Jones vector E_0 of the output beam can be written as

$$E_0 = P(\theta_p)R(\theta_5)C(\delta)R(\theta_4 - \theta_5)C(\delta)R(\theta_3 - \theta_4) \\ \times C(\delta)R(\theta_2 - \theta_3)C(\delta)R(\theta_1 - \theta_2) \\ \times C(\delta)R(-\theta_1)P(0)E_i, \quad (3)$$



(m)



(n)

where E_i is the Jones vector of the input beam as shown in Sec. III.

We now study the effect of inserting rotator plates of different thickness in a five-stage linear birefringent network having an approximated periodic triangular amplitude transmittance. The azimuths of linear retarders and output polarizer of a linear birefringent network having an approximated periodic triangular amplitude transmittance are given by³

$$\begin{aligned} \theta_1 &= 88^\circ 45', & \theta_2 &= 84^\circ 52', & \theta_3 &= 55^\circ 31', \\ \theta_4 &= 26^\circ 10', & \theta_5 &= 22^\circ 18', & \theta_p &= 21^\circ 3', \end{aligned} \quad (4)$$

substituting the values of the Eqs. (4) in expression (3) we get the T vs λ curve of Fig. 8 by the direct matrix multiplication (as in Sec. III). At $\lambda = 509$ nm each retarder behaves as a full wave plate and we get the intensity maxima at this wavelength.

If now the slow axis of each retarder is made parallel to the transmission axis of the input polarizer $P(0)$ and the rotator plates are placed in such a way that the first rotator $R(\alpha_1)$ rotates the plane of polarization of the spectral com-

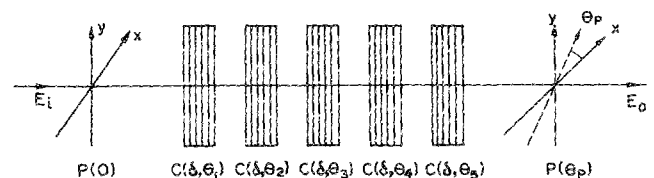


FIG. 7. Diagram shows a five-stage generalized linear birefringent network where $C(\delta, \theta)$ represents a linear retarder having a frequency-dependent retardance δ and azimuth θ . $P(\theta_p)$ represents a linear polarizer with an azimuth θ_p .

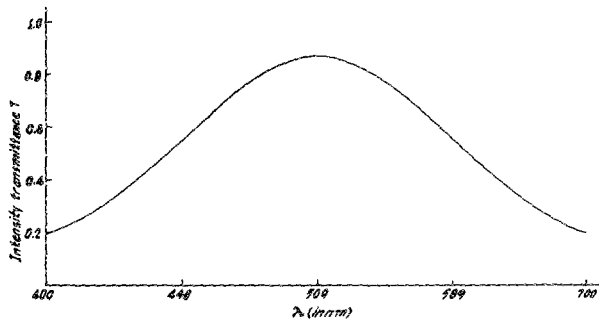


FIG. 8. Curve shows the variation of intensity transmittance T with wavelength λ of a five-stage linear birefringent network having an approximated periodic triangular amplitude transmittance.

ponent $\lambda = 509$ nm through the angle $-\theta_1$ deg, the second rotator $R(\alpha_2)$ rotates the plane of polarization of $\lambda = 509$ nm through an angle $(\theta_1 - \theta_2)$ deg, and so on, the Jones vector E_0 of the output beam can be written with the help of expression (3) as

$$E_0 = P(\theta_p)R(\alpha_6)C(\delta)R(\alpha_5)C(\delta)R(\alpha_4) \\ \times C(\delta)R(\alpha_3)C(\delta)R(\alpha_2)C(\delta)R(\alpha_1)P(0)E_i. \quad (5)$$

The arrangement of the elements of the network that corresponds to expression (5) is shown in Fig. 9. With the help of Biot's law the thickness of rotators $R(\alpha_1), R(\alpha_2), R(\alpha_3), R(\alpha_4), R(\alpha_5)$, and $R(\alpha_6)$ are obtained as $t_1 = 3$ mm, $t_2 = 0.13$ mm, $t_3 = 1$ mm, $t_4 = 1$ mm, $t_5 = 0.13$ mm, and $t_6 = 0.76$ mm, respectively, for $\lambda = 509$ nm as the tuning wavelength. Here the rotator $R(\alpha_1)$ rotates the plane of polarization of the wavelength components through the clockwise direction and all other rotators intro-

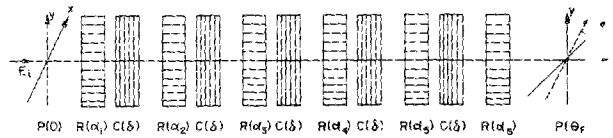


FIG. 9. Diagram shows a birefringent network where the slow axis of each retarder is parallel to the transmission axis of the input polarizer and the rotators of different thickness are used as interstage elements.

duce anticlockwise rotation. Plot (a) of Fig. 10 shows the T vs λ curve of the network (Fig. 9) for different rotator thickness shown above and for the same thickness of each retarder plate. Comparing the T vs λ curve of Fig. 8 with that of plot (a) of Fig. 10 we notice a marked difference between the two distributions. Although the intensity transmittances at $\lambda = 509$ nm are same in both the cases, plot (a) of Fig. 10 shows an increase at lower wavelength side and rather sharp decrease at higher wavelength side of $\lambda = 509$ nm, showing a more or less flat-top intensity transmittance over a wide range of visible region. If now we tune the network at some higher wavelength $\lambda = 546$ nm, the T vs λ curve thus obtained is shown in plot (b) of Fig. 10. At $\lambda = 546$ nm each retarder behave as a full wave plate and the thickness of the rotators are obtained as $t_1 = 3.5$ mm, $t_2 = 0.15$ mm, $t_3 = 1.16$ mm, $t_4 = 1.16$ mm, $t_5 = 0.15$ mm, and $t_6 = 0.88$ mm. Here again the first rotator introduces clockwise rotation and all other rotators introduce anticlockwise rotation. Similarly tuning the network at some lower wavelength $\lambda = 432$ nm, the rotators thicknesses are obtained as $t_1 = 2$ mm (right-handed rotator), $t_2 = 0.1$ mm, $t_3 = 0.71$ mm, $t_4 = 0.71$ mm, $t_5 = 0.10$ mm, and $t_6 = 0.54$ mm. The T vs λ curve thus obtained is shown in plot (c) of Fig. 10. The curve resembles that of a band suppression one with large band-

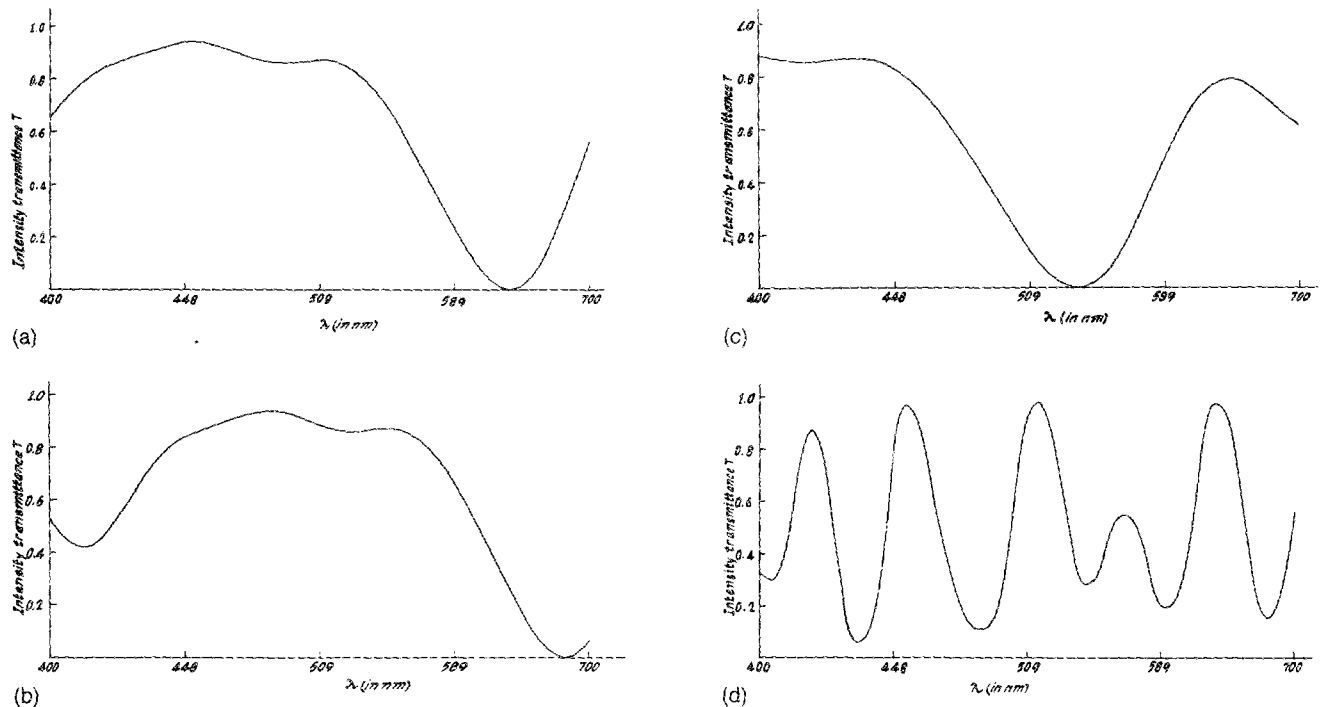


FIG. 10. Plots (a)–(d) show the transmission curves of birefringent filter system where the thickness of the elements of the successive stages are different.

width tuned at the principal rejection wavelength at $\lambda = 530$ nm.

In the network configurations discussed above we see that the first rotator introduces a clockwise rotation. If now we change the first right-hand rotator by a left-handed rotator which rotates the plane of polarization of the wavelength component $\lambda = 509$ nm through an angle $(360 - \theta_1)$ deg in the anticlockwise direction, the T vs λ curve thus obtained (using other rotators as used for tuning at $\lambda = 509$ nm) is shown in plot (d) of Fig. 10. In this case the thickness of the first left-handed rotator is $t_1 = 2.7$ cm.

Plot (d) of Fig. 10 shows the T vs λ curve of a multi-bandpass filter with maxima at $\lambda = 418, 453, 516, 563,$ and 629 nm. The peaks of all these maximas do not attain the ideal value of full transmission. The peaks at $\lambda = 453, 516,$ and 629 nm attain 98% where as the peaks at $\lambda = 418$ and 563 nm attain 89% and 55%, respectively, of their ideal

value of full transmission. Similarly we also note that the minima do not attain their ideal value of zero transmission. However, any properly tuned band suppression filter can be combined to this set up for complete suppression of any desired wavelength.

ACKNOWLEDGMENTS

The author acknowledges the valuable guidance by Dr. A. K. Chakraborty, Reader, Department of Applied Physics and sincere cooperation by the members of the staff of the Department of Computer Science, Calcutta University.

¹B. Chakraborty, *J. Appl. Phys.* **59**, 3356 (1986).

²E. O. Ammann, *Prog. Opt.* **9**, 123 (1971).

³S. E. Harris, E. O. Ammann, and I. C. Chang, *J. Opt. Soc. Am.* **54**, 1267 (1964).